Am J Cancer Res 2016;6(2):141-156
www.ajcr.us /ISSN:2156-6976/ajcr0016806

Original Article

MicroRNA-10b regulates epithelial-mesenchymal transition by modulating KLF4/Notch1/E-cadherin in cisplatin-resistant nasopharyngeal carcinoma cells

Pei Zhang[1*], Haiyu Hong[2*], Xiaojin Sun[1*], Hao Jiang[3], Shiyin Ma[4], Surong Zhao[1], Mengxiao Zhang[1], Zhiwei Wang[5,6], Chenchen Jiang[1,7], Hao Liu[1]

[1]Faculty of Pharmacy, Bengbu Medical College, Anhui Engineering Technology Research Center of Biochemical Pharmaceuticals, Bengbu 233030, Anhui, P. R. China; [2]Department of Otolaryngology, The Fifth Affiliated Hospital of Sun Yat-sen University, Zhuhai 519000, China; [3]Department of Radiotherapy, The First Affiliated Hospital of Bengbu Medical College, No 287, Chang-Huai Road, Bengbu 233000, Anhui, P. R. China; [4]Department of ENT, The First Affiliated Hospital of Bengbu Medical College, No 287, Chang-Huai Road, Bengbu 233000, Anhui, P. R. China; [5]Department of Pathology, Beth Israel Deaconess Medical Center, Harvard Medical School, Boston, MA 02215, USA; [6]The Cyrus Tang Hematology Center and Collaborative Innovation Center of Hematology, Jiangsu Institute of Hematology, The First Affiliated Hospital, Soochow University, Suzhou, China; [7]Priority Research Center for Cancer Research, University of Newcastle, Newcastle, NSW 2308, Australia. [*]Equal contributors.

Received September 24, 2015; Accepted December 21, 2015; Epub January 15, 2016; Published February 1, 2016

Abstract: Epithelial-mesenchymal transition (EMT) is an initiating event in tumor cell invasion and metastasis that contributes to therapeutic resistance to compounds including cisplatin. MicroRNAs (miRNAs) have been associated with EMT as well as resistance to standard therapies. However, the underlying mechanisms by which miRNAs control the development of resistance to cisplatin (DDP), and the accompanying EMT-like properties are required to elucidate. Here we show that microRNA-10b (miR-10b) is up-regulated in HNE1/DDP cells, and inhibition of miR-10b expression reversed the EMT phenotype. However, over-expression of miR-10b was able to promote the acquisition of an EMT phenotype in HNE1 cells. Additionally, we identified that miR-10b expression inversely correlates with KLF4, which then controls expression of Notch1. Knock-down of Notch1 inhibited cell migration, invasion, and reversed EMT in HNE1/DDP cells, which was dependent on miR-10b. In summary, our results reveal that miR-10b regulates EMT by modulating KLF4/Notch1/E-cadherin expression, which promotes invasion and migration of nasal pharyngeal carcinoma cells.

Keywords: miR-10b, EMT, Notch1, invasion, KLF4, miRNA

Introduction

Nasopharyngeal carcinoma (NPC) is a prevalent head and neck cancer common in Southeast Asia and China, with an incidence rate of approximately 20-50 cases per 100,000 individuals per year [1]. Radiotherapy is the primary therapeutic course of action, and when combined with chemotherapy is an effective treatment against advanced carcinoma [2]. With the improvement of diagnostic and therapeutic approaches, most patients with early-stage NPC have been cured successfully. However, the 5-year survival rate of most middle-late and late-stage patients is extremely low, with treatment failure primarily due to the development of drug resistance and metastasis to distant organs.

MicroRNAs (miRNAs) are highly conserved single-stranded small non-coding RNA molecules about 18-25 nucleotides in length. They regulate physiological processes post-transcriptionally by binding to complementary target sequences in the 3' untranslated regions (3' UTRs) of mRNAs causing translational repression and/or mRNA destabilization [3]. It has been proposed that miRNAs are involved in embryonic development, tumorigenesis, metastasis, metabolism, and many other physiologi-

Table 1. Transfected gene sequences

Gene	Sequence (5'→3')
Negative control	sense UUCUCCGAACGUGUCACGUTT
	anti-sense ACGUGACACGUUCGGAGAATT
miR-10b mimics	sense UACCCUGUAGAACCGAAUUUGUG
	anti-sense CAAAUUCGGUUCUACAGGGUAUU
miRNA inhibitor NC	CAGUACUUUUGUGUAGUACAA
miR-10b inhibitor	CACAAAUUCGGUUCUACAGGGUA
siControl	sense UUCUCCGAACGUGUCACGUTT
	anti-sense ACGUGACACGUUCGGAGAATT
siNotch1-A	sense GUCCAGGAAACAACUGCAATT
	anti-sense UUGCAGUUGUUUCCUGGACTT
siNotch1-B	sense CAGGGAGCAUGUGUAACAUTT
	anti-sense AUGUUACACAUGCUCCCUGTT
siNotch1-C	sense GGGCUAACAAAGAUAUGCATT
	anti-sense UGCAUAUCUUUGUUAGCCCTT

cal and pathological processes [4]. Although the biological functions of most miRNAs have not been fully elucidated, the involvement of miRNAs in drug resistance and epithelial-mesenchymal transition (EMT) has been recently reported [5]. Some miRNAs have oncogenic activity and are up-regulated in cancer, whereas others have tumor suppressor activity and are down-regulated in cancer [6]. Moreover, miRNAs have been implicated in the process of EMT through the modulation of EMT-related genes [7]. However, a role for miRNAs in regulating resistance to cisplatin as well as the accompanying EMT-like properties leading to a higher invasive capacity of NPC has yet to be reported.

EMT has been characterized as a multi-step event involving various key signaling pathways including the TGF-β, EGF, NF-κB, Wnt, and Notch pathways [8]. New evidence shows that Notch signaling promotes EMT by converting polarized epithelial cells into motile, invasive cells during tumor progression [9]. Moreover, multiple studies have suggested that Notch1 plays a key role in the regulation of EMT during the development and progression of pancreatic tumors, resulting in tumor recurrence and development of drug resistance in pancreatic cancer [10]. However, the role of Notch1 signaling in NPC is not well understood. In this study, we demonstrate that cisplatin resistant cells with an EMT phenotype have up-regulation of miR-10b, resulting in down-regulation of KLF4 and subsequent up-regulation of Notch1.

Materials and methods

Reagents and antibodies

Cisplatin (DDP) was purchased from Qilu Pharmaceutical Co., Ltd. (Jinan, China). RPMI-1640 medium, fetal bovine serum (FBS) and phosphate-buffered saline (PBS) were purchased from Gibco-BRL (grand Island, NY, USA). Matrigel was purchased from BD Biosciences (Bedford, MA, USA). Primary antibodies against E-cadherin, Vimentin, MMP-9 (1:500), and β-actin (1:800) were obtained from Santa Cruz Biotechnology (Santa Cruz, CA, USA). Anti-Notch1 antibody was obtained from Abcam (MA, USA).

Cell lines and cell transfection

HNE1 and HNE1/DDP cells were grown in RPMI-1640 medium containing 10% FBS with penicillin (100 U/mL) and streptomycin (100 U/mL) at 37°C with 5% CO_2. The RPMI-1640 medium for culturing HNE1/DDP cells was supplemented with DDP (4 μmol/L). All cell lines were tested each month for mycoplasma contamination, used only at low passage, and regularly examined under a microscope for phenotypic changes prior to use. Negative control mimics (NC), miR-10b mimics (miR-10b), miR-10b inhibitors (anti-miR-10b), negative control inhibitors (anti-NC), and Notch1 siRNAs (for sequences, see **Table 1**) were synthesized by GenePharma Company (Shanghai, China). The Notch1 cDNA plasmid was previously described [11]. Transfections were performed with Lipofectamine 2000 (Invitrogen, CA, USA) according to the manufacturer's protocol. Total RNAs and proteins were prepared at 48 h post transfection for qRT-PCR analysis or Western blotting, respectively.

Morphological analysis

Cells were grown to 70% confluence in DDP-free medium for HNE1 cells and in medium supplemented with DDP for HNE1/DDP cells. Cells were visualized under light microscopy (CKX41; Olympus, Tokyo, Japan). Images were captured using a microscope mounted digital camera (CellSens Entry; Olympus).

Wound healing assay

Cell migration was assessed using a wound healing assay. The HNE1 and HNE1/DDP cells

Table 2. Primer sequences used for qRT-PCR

Gene	Primer sequence (5'→3')
E-cadherin	F: CATTTCCCAACTCCTCTCCTGGC
	R: ATGGGCCTTTTTCATTTTCTGGG
Vimentin	F: AGATGGCCCTTGACATTGAG
	R: TGGAAGAGGCAGAGAAATTC
MMP9	F: CGGAGTGAGTTGAACCAG
	R: GTCCCAGTGGGGATTTAC
Notch1	F:CTTTGTGCTTCTGTTCTTCGTG
	R:ACTCATTCTGGTTGTCGTCCAT
GAPDH	F:CAGCCTCAAGATCATCAGCA
	R:TGTGGTCATGAGTCCTTCCA

were seeded into a 6-well plate (Corning Life Sciences) and allowed to grow to 70% confluence. Cells were then scraped with a sterile micropipette tip to create a gap of standard width and then washed several times with PBS to remove cell debris. The gap closure was observed under an inverted microscope after 24 h, imaged and gap measured to calculate healing percentages.

Invasion and migration assay

The ability of the cells to pass through filters was measured using a Transwell Boyden chamber system (Corning Life Sciences) containing a poly-carbonate filter (6.5 mm in diameter, 8 μm pore size). For cell invasion assays, the membrane undersurface was coated with 50 μL of Matrigel mixed with RPMI-1640 serum-deprived medium at a 1:8 dilution and subsequently applied to the top side of the filter. By contrast, the filter was not coated for the cell migration assay. In both assays, cell suspensions (5×10^4 cells/well) were added to the upper chamber in medium without serum. Medium containing 10% FBS in the lower chamber served as a chemo-attractant. The cells that did not migrate or invade after 24 h of incubation were removed from the upper face of the filters by scrubbing with a cotton swab. Membranes were then fixed with 4% formaldehyde for 15 min at room temperature and stained with 0.5% crystal violet for 15 min. Finally, the number of migrating or invading cells was counted at ×200 magnification from ten different fields for each filter and analyzed to determine statistically significance. The experiments were performed in triplicate and the results were expressed as the number of cells per field.

Western blot analysis

Cells were plated in 6-well culture dishes (Corning Life Sciences) at a density of 4×10^5 cells/well. Following 24 h of incubation, the cells were washed with 1 mL PBS/well and harvested by trypsin. cell lysates were centrifuged at 12,000 rpm for 30 min at 4°C, following incubation on ice for 30 min in lysis buffer. Protein concentrations were determined using the bicinchoninic acid (BCA) assay (Beyotime Institute of Biotechnology, Beijing, China). Subsequently, total protein (50 μg) was separated using 8-15% sodium dodecyl sulfate-polyacrylamide gel electrophoresis (SDS-PAGE) and transferred onto polyvinylidene difluoride (PVDF) membranes. The membranes were blocked with 5% nonfat dried milk in TBS-T (20 mmol/L Tris, 0.15 mol/L NaCl (pH 7.0), 0.1% Tween 20) for 2 h, and probed with primary antibodies overnight at 4°C. The membranes were then washed and incubated with HRP-conjugated secondary antibody and finally visualized with Chemiluminescent ECL reagent (Millipore, MA, USA). The membranes were imaged with gel imaging equipment (Bio-Rad, Hercules, CA, USA).

miRNA analysis

For miRNA analysis, total RNA was isolated using the miRNeasy Mini Kit (Qiagen) following the manufacturer's instructions, and the RNA concentration was determined by NanoVue™ Plus (Thermo Fisher Scientific, Inc., GE Healthcare, USA). Aliquots (1 μg) of total RNA were converted to cDNA using miScript II RT Kit (Qiagen). Diluted cDNA was mixed with miScript SYBR Green PCR Kit (Qiagen) containing universal primers and SYBR Green dye and added to the wells of 96-well plates containing lyophilized primer. The plates were run on an ABI StepOne™ Real-Time PCR System (Applied Biosystems, Foster City, CA, USA) and the expression of individual miRNAs was analyzed using the determined Ct values. The fold change for each miRNA was calculated by using the Crossing point (Cp) values and the manufacturer's web-based software. HNE1 cells were considered control cells for the comparison of fold change in HNE1/DDP cells. U6 was used as an endogenous control to normalize the Ct values obtained for each gene. Changes in gene expression were calculated using the using the $2^{-\Delta\Delta Ct}$ method.

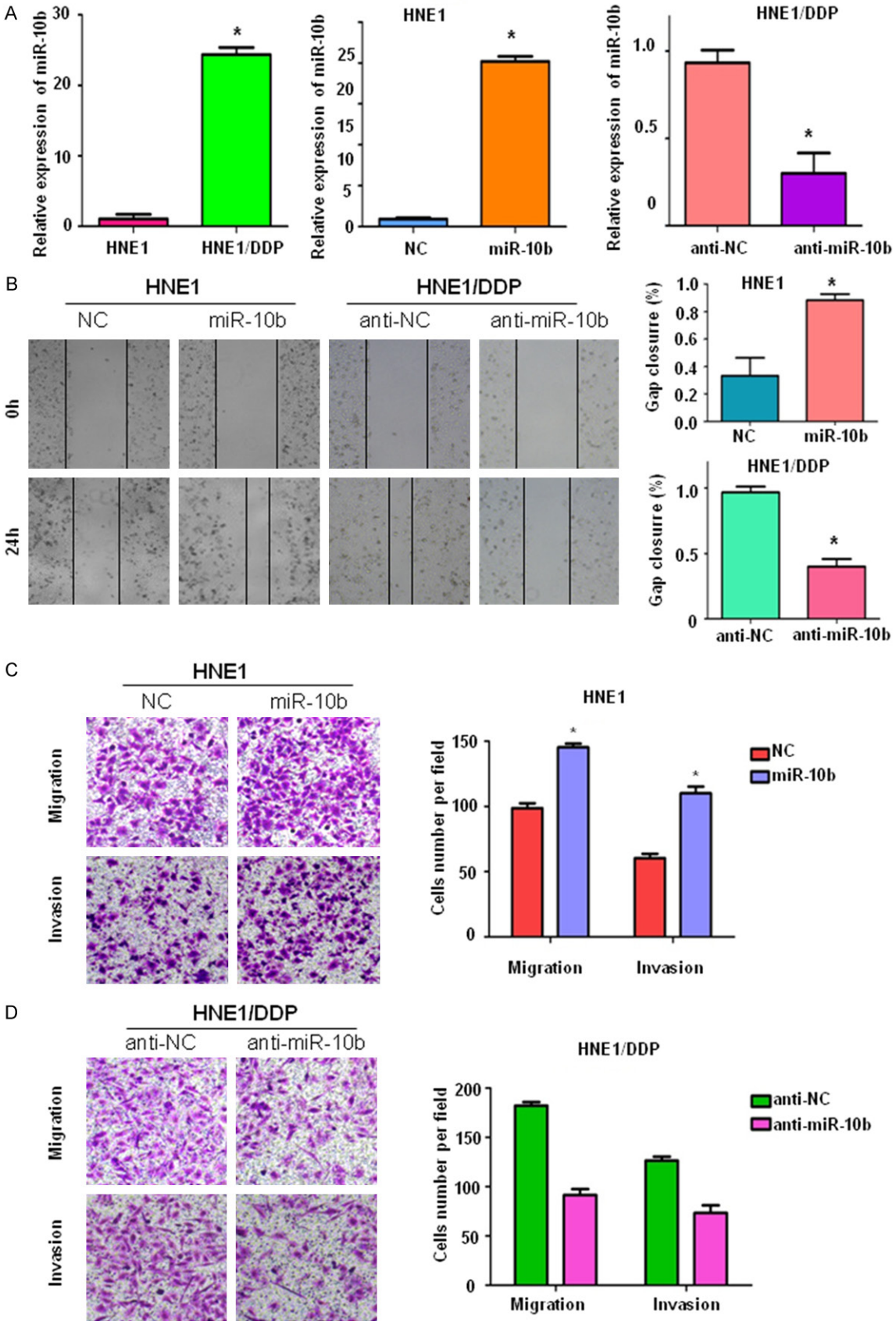

Figure 1. miR-10b promotes the migration and invasion of HPC cells. A. Left panel: qRT-PCR analysis of miR-10b expression in HNE1 and HNE1/DDP cells. The relative amount of miRNA was normalized to U6 (Mean ± SEM, *P<0.05

compared to parental HNE1 cells). Middle panel: HNE1 cells transfected with miR-10b mimics. Relative levels of miR-10b were analyzed 48 h post transfection by qRT-PCR analysis (Mean ± SEM, *P<0.05 compared to NC). Right panel: HNE1/DDP cells were transfected with miR-10b inhibitors. Relative levels of miR-10b were analyzed 48 h post transfection by qRT-PCR analysis (Mean ± SEM, *P<0.05 compared to anti-NC). B. Left panel: Wound healing assays comparing the migratory potential of HNE1 or NHE1/DDP cells transfected with miR-10b mimics or anti-miR-10b, respectively (images acquired at 100× magnification). Right panel: Quantification of gap closure (Mean ± SEM, *P<0.05 compared to NC). C. Left panel: Transwell Boyden chamber assays to compare the migratory and invasive potential of HNE1 cells transfected miR-10b mimics (images acquired at 200× magnification). Right panel: Quantification of migrated and invaded cells (Mean ± SEM, *P<0.05 compared to NC). D. Left panel: Transwell Boyden chamber assays to compare the migratory and invasive potential of HNE1/DDP cells transfected miR-10b inhibitors (images acquired at 200× magnification). Right panel: Quantification of migrated and invaded cells (Mean ± SEM, *P<0.05 compared to anti-NC).

Quantitative mRNA analysis

Total RNA was isolated using TRIzol reagent (Invitrogen Life Technologies, Carlsbad, CA, USA) and RNA concentration was determined by NanoVue™ Plus. Aliquots (1 μg) of total RNA were reverse transcribed to cDNA (20 μL) using oligo(dT) and M-MuLV reverse transcriptase (Fermentas Inc., glen Burnie, MD, USA) following the manufacturer's protocol. Diluted cDNA was used as a template for PCR using the SYBR®-Green PCR kit (Takara, Kyoto, Japan) in an ABI StepOne™ Real-Time PCR System. The housekeeping gene, glyceraldehyde-3-phosphate dehydrogenase (GAPDH), was selected as an internal control for each experiment. The primers used in this study are presented in **Table 2**. All reactions were run in triplicate, ΔΔCt values were calculated and converted to approximate fold change values ($2^{-\Delta\Delta Ct}$).

Statistical analysis

Data are presented as the mean ± SEM. The p value between mean values was calculated using the two-tailed Student's t-test. All statistical analyses were performed using SPSS 13.0 software (SPSS Inc., Chicago, IL, USA). P values <0.05 were considered to indicate statistical significance.

Results

Expression of miR-10b in HNE1/DDP cells

In order to identify whether miR-10b was involved in the underlying mechanisms of cisplatin resistance and induction of EMT-like properties, we first assessed the expression of miR-10b in the cisplatin-resistance cell line HNE1/DDP compared with the parental HNE1 cell line. We found that miR-10b was up-regulated about 25-fold in HNE1/DDP compared with HNE1 cells by qRT-PCR (**Figure 1A**, left panel). To determine whether miR-10b mimics could function *in vitro*, the HNE1 cell line, which expressed lower levels of miR-10b, was transfected with miR-10b mimics. We observed that expression of miR-10b was dramatically increased following transfection of the miR-10b mimics (**Figure 1A**, middle panel). Likewise, to reduce expression of miR-10b in HNE1/DDP cells, which showed higher levels of miR-10b, we transfected miR-10b inhibitors, which dramatically reduced miR-10b level (**Figure 1A**, right panel). These results indicate that miR-10b mimics and inhibitors can be successfully transfected into nasopharyngeal carcinoma cells to alter the levels of miR-10b.

MiR-10b promotes the migration and invasion of human NPC cells

Based on the above results, we tested whether miR-10b could change the migration and invasion capacity of human NPC cells using wound healing and Transwell Boyden chamber assays. We found that wound healing was enhanced in HNE1 cells transfected with miR-10b mimics (**Figure 1B**, HNE1 cells) and reduced in HNE1/DDP cells by miR-10b inhibitors compared to control transfection conditions (**Figure 1B**, NHE1/DDP cells). In addition, the relative number of cells undergoing migration and invasion were increased by miR-10b mimics (**Figure 1C**), and decreased by miR-10b inhibitors as compared to control cells (**Figure 1D**). These results indicate a positive role for miR-10b in the migration and invasion of human NPC cells.

MiR-10b regulates EMT in human NPC cells

Morphological analysis indicates that HNE1 cells transfected with miR-10b mimics exhibited a greater number of mesenchymal cells (**Figure 2A**). In contrast, inhibition of miR-10b expression reversed the EMT phenotype of HNE1/DDP cells (**Figure 2A**). To fully explore

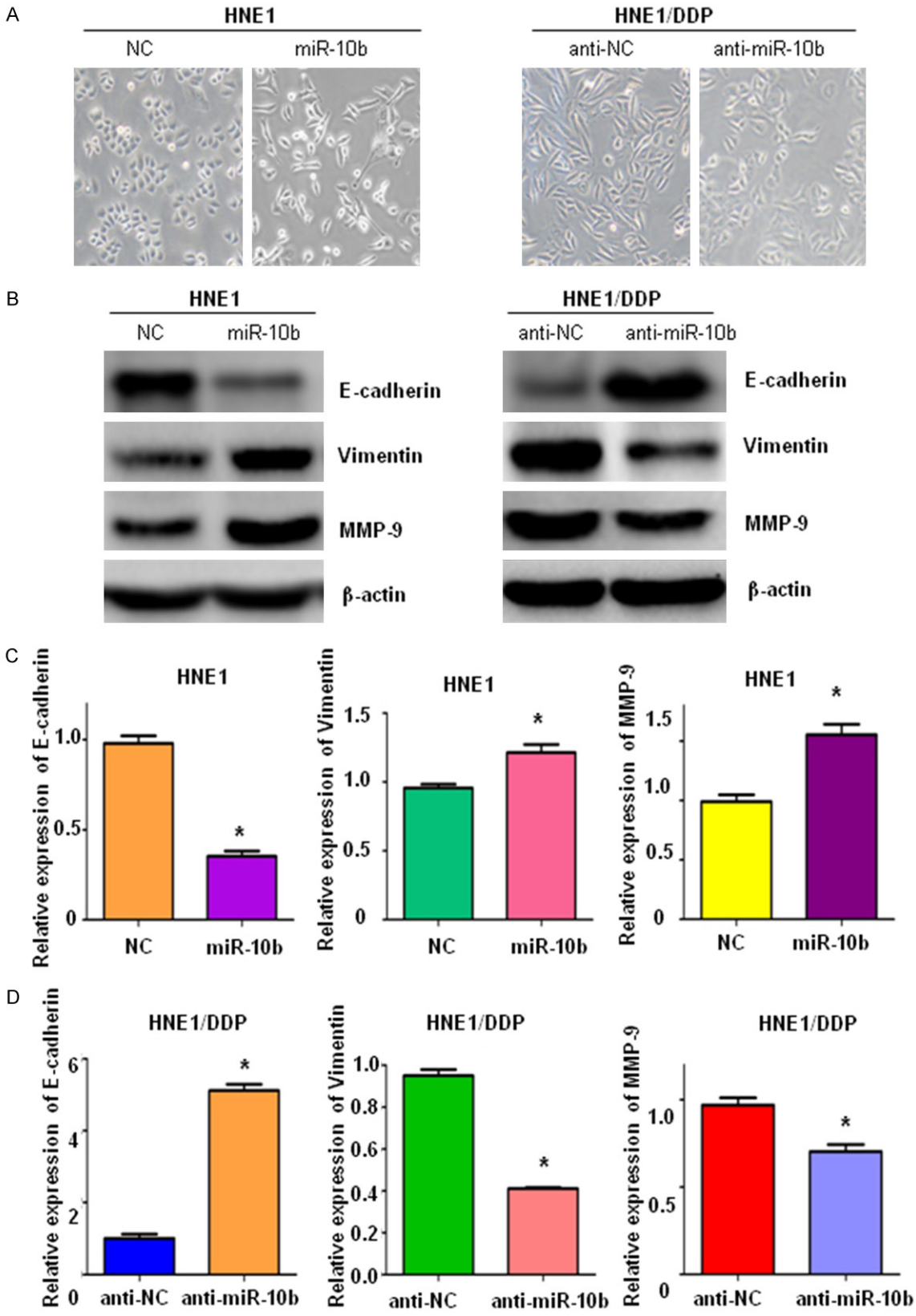

Figure 2. miR-10b regulates EMT in human NPC cells. A. Cell morphology of HNE1 cells following transfection with miR-10b mimics and in HNE1/DDP cells following transfection with miR-10b inhibitors (images acquired at 200× magnification). B. Western blot analysis demonstrating that miR-10b mimics reduce E-cadherin protein abundance but enhanced vimentin and MMP9 protein abundance in HNE1 cells. In contrast, miR-10b inhibitors promoted E-

cadherin protein abundance but decreased vimentin and MMP9 protein abundance in HNE1/DDP cells. C. qRT-PCR analysis demonstrating that expression of E-cadherin was down-regulated, whereas vimentin and MMP9 expression were up-regulated in HNE1 cells following transfection of miR-10b mimics. The relative amount of mRNA was normalized to GAPDH (mean ± SEM, *P<0.05 compared to NC). D. qRT-PCR analysis demonstrating that expression of E-cadherin was up-regulated, whereas vimentin and MMP9 expression were down-regulated in HNE1/DDP cells following transfection with miR-10b inhibitors (Mean ± SEM, *P<0.05 compared to anti-NC).

the role of miR-10b in the regulation of EMT in HNE1 and HNE1/DDP cells, we measured the expression levels of EMT-related proteins following transfection with miR-10b mimics or inhibitors in HNE1 or HNE1/DDP cells, respectively. We observed a decrease of E-cadherin at both the protein and mRNA levels in response to transfection of HNE1 cells with miR-10b mimics (**Figure 2B**, **2C**). Vimentin and MMP9 were increased in protein and mRNA abundance (**Figure 2B**, **2C**). Similar to our observations of changes in cellular morphology (**Figure 2A**), transfection of HNE1/DDP cells with miR-10b inhibitors had the opposite effect, showing an increase in E-cadherin and decrease in vimentin and MMP9 protein abundance and mRNA expression (**Figure 2B** and **2D**). Altogether, these results demonstrate that miR-10b plays an important role in the regulation of EMT in human NPC cells.

MiR-10b regulates KLF4 in human NPC cells

KLF4 has previously been shown to be down-regulated in human esophageal cancer [12, 13] and correlates with cancer metastasis [14]. Furthermore, KLF4 is a putative target of miR-10b in esophageal cancer [15], and recent studies have shown that KLF4 negatively regulates EMT in gastrointestinal cancer [16]. Therefore, to determine if miR-10b regulates KLF4 expression, we assessed the KLF4 protein and mRNA levels in HNE1 and HNE1/DDP cells. Consistent with the increase in miR-10b, we observed a reduction in mRNA and protein levels of KLF4 in HNE1/DDP cells compared to HNE1 cells (**Figure 3A**). Previous results have also demonstrated that KLF4 regulates the Notch signaling pathway [17]. Consistent with differential KLF4 abundance in HNE1 versus HNE1/DDP cells, we detected the mRNA and protein levels of Notch1 were higher in HNE1/DDP cells compared to HNE1 cells (**Figure 3B**). Moreover, we found that expression of KLF4 was significantly reduced in HNE1 cells transfected with miR-10b mimics, but KLF4 was increased in HNE1/DDP cells transfected with miR-10b inhibitors (**Figure 3C**, **3D**). We also observed that transfection of NHE1 cells with miR-10b mimics resulted in increased Notch1 (**Figure 3C**). Moreover, transfection of HNE1/DDP cells with miR-10b inhibitors decreased the level of Notch1 (**Figure 3D**). Our results indicate that the levels of KLF4 are reduced by miR-10b, which induces Notch1 signaling.

Knockdown of Notch1 decreases cell migration and invasion

Given that we have demonstrated the Notch1 is under the control of miR-10b through regulation of KLF4, we next wanted to determine if depletion of Notch1 influenced migration and invasion in a similar manner to depletion of miR-10b. To determine the effect of Notch1 on migration and invasion in HNE1/DDP cells, we depleted Notch1 expression with small interfering RNAs (siRNAs). The protein and mRNA levels of Notch1 were both decreased 48 h following siRNA transfection (**Figure 4A**). Moreover, the wound healing capacity of HNE1/DDP cells was reduced after treatment with Notch1 siRNA (**Figure 4B**). Furthermore, the relative number of HNE1/DDP cells undergoing migration and invasion was decreased following Notch1 depletion (**Figure 4C**). These results indicate that down-regulation of Notch1 could suppress the migration and invasion of human NPC cells, suggesting that the ability of miR-10b to control migration and invasion is through regulating KLF4 and Notch1.

Knockdown of Notch1 reverses EMT in HNE1/DDP cells

Next, we set out to determine whether Notch1 could regulate the expression levels of EMT-related molecules in HNE1/DDP cells. Based on morphological analysis we found that HNE1/DDP cells transfected with Notch1 siRNA shifted from a mesenchymal-like spindle-cell shape to an epithelial-like appearance (**Figure 5A**). Moreover, the mRNA and protein levels of E-cadherin were increased while the mRNA and protein levels of vimentin and MMP9 were decreased in response to Notch depletion (**Figure 5B**, **5C**). These results suggest that depletion of Notch1 expression can reverse EMT in

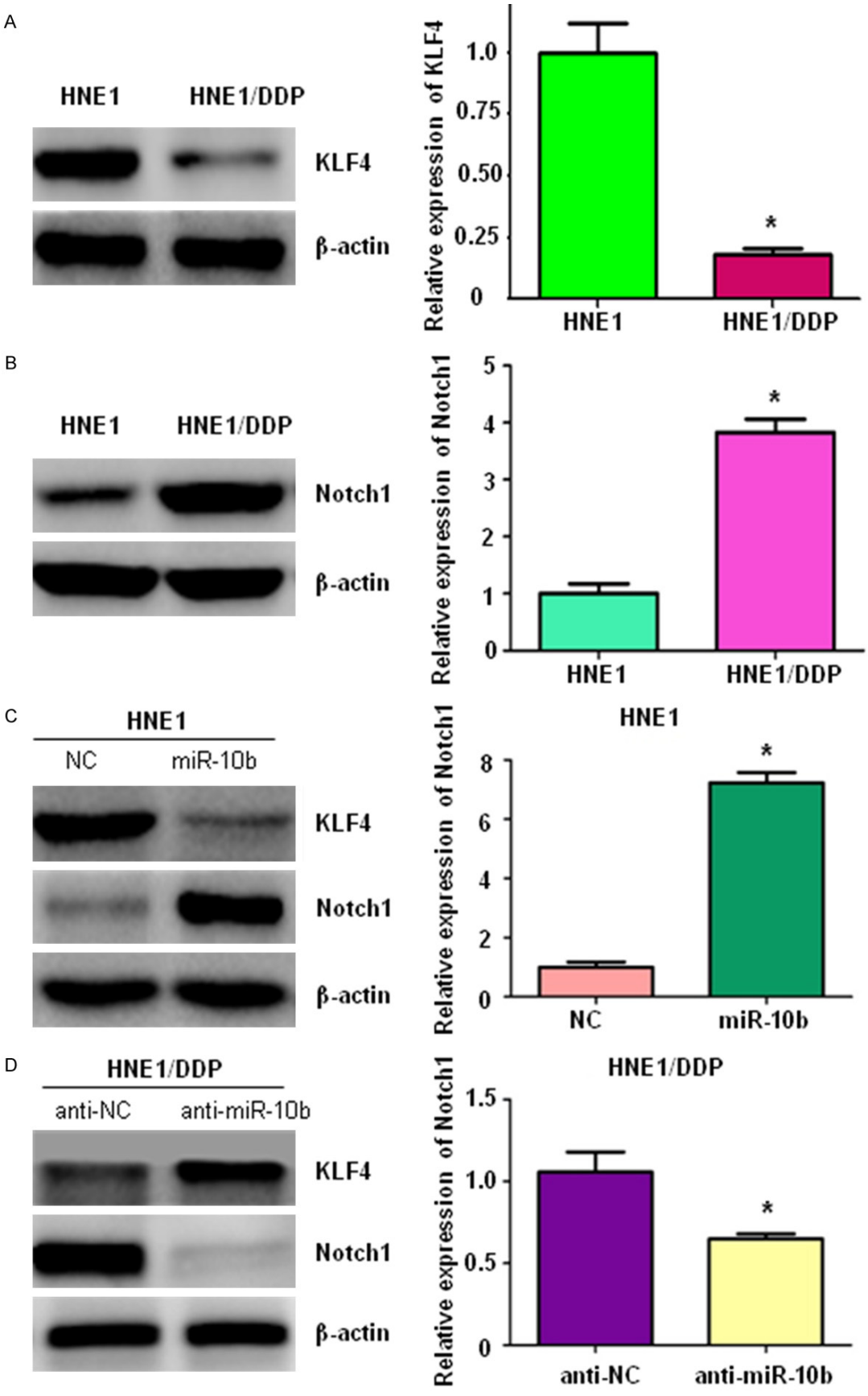
A
HNE1
HNE1/DDP
KLF4
β-actin
Relative expression of KLF4
1.0
0.75
0.50
0.25
0
*
HNE1
HNE1/DDP
B
HNE1
HNE1/DDP
Notch1
β-actin
Relative expression of Notch1
5
4
3
2
1
0
*
HNE1
HNE1/DDP
C
HNE1
NC
miR-10b
KLF4
Notch1
β-actin
Relative expression of Notch1
8
6
4
2
0
*
NC
miR-10b
D
HNE1/DDP
anti-NC
anti-miR-10b
KLF4
Notch1
β-actin
Relative expression of Notch1
1.5
1.0
0.5
0
*
anti-NC
anti-miR-10b

Figure 3. miR-10b regulates KLF4 in human NPC cells. A. Protein and mRNA levels of KLF4 were reduced in HNE1/DDP cells compared with HNE1 cells (Mean ± SEM, **P*<0.05 compared with parental HNE1 cells). B. Protein and mRNA levels of Notch1 were higher in HNE1/DDP cells compared with HNE1 cells (Mean ± SEM, **P*<0.05 compared with parental HNE1 cells). C. Left panel: Western blot analysis demonstrating that miR-10b mimics reduced KLF4 protein expression, leading to enhanced Notch1 expression in HNE1 cells. Right panel: qRT-PCR analysis reveals that Notch1 mRNA level was increased in HNE1 cells transfected with miR-10b mimics. D. Left panel: miR-10b inhibitors promoted KLF4 protein abundance, leading to a decrease in Notch1 protein level in HNE1/DDP cells by Western blot analysis. Right panel: qRT-PCR analysis reveals that the mRNA level of Notch1 was down-regulated by miR-10b inhibitors transfection (mean ± SEM, **P*<0.05 compared to anti-NC).

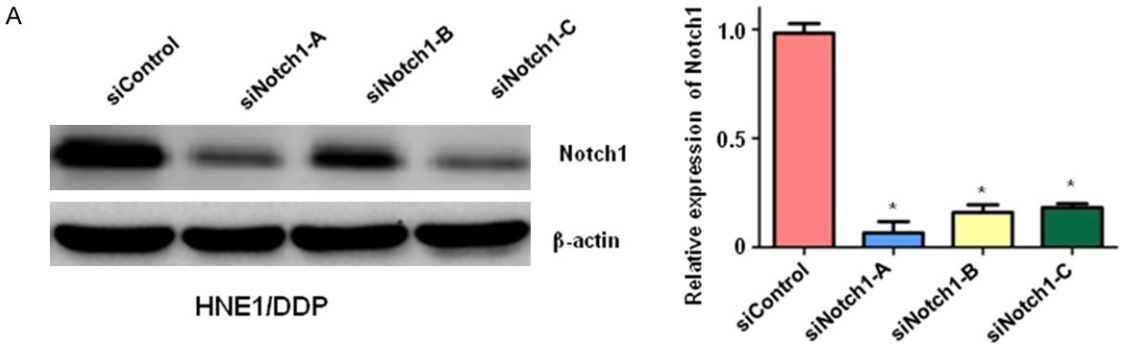

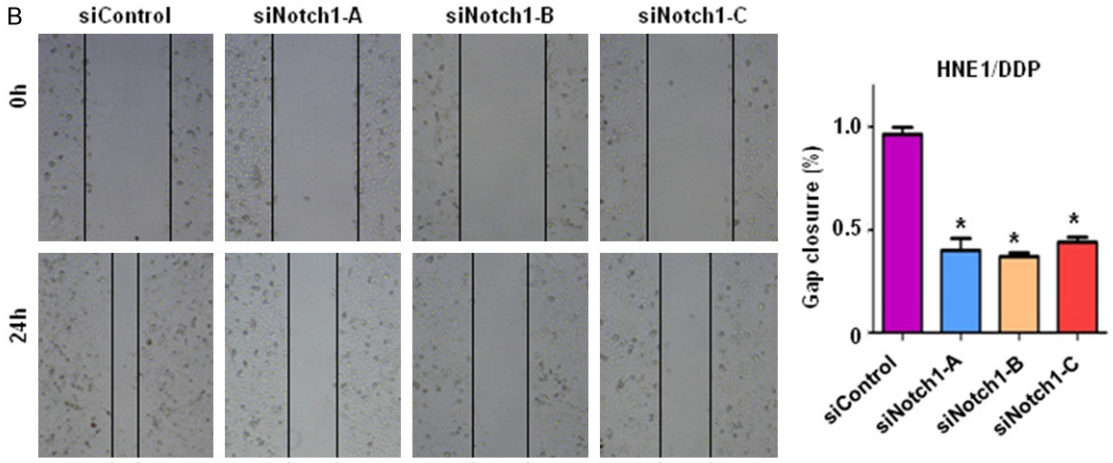

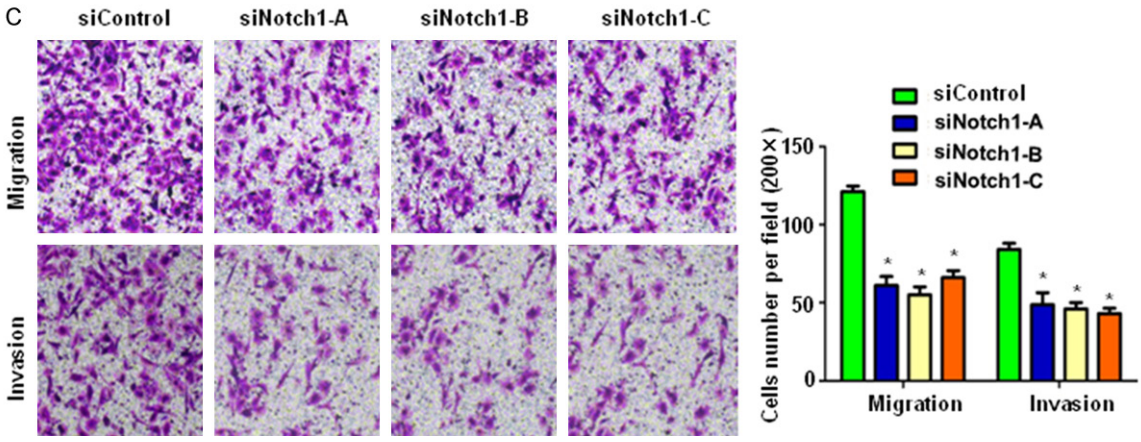

Figure 4. Knockdown of Notch1 decreases cell migration and invasion in HNE1/DDP cells. A. Left panel: HNE1/DDP cells transfected with control or Notch1 siRNA. Whole-cell lysates harvested 48 h post transfection was subjected to western blot analysis. Right panel: qRT-PCR analysis of Notch1 expression in HNE1/DDP cells after control or Notch1 siRNA transfection. mRNA was normalized to GAPDH (Mean ± SEM, **P*<0.05, compared to siControl). B. Left panel: Wound healing assays to determine migratory potential of HNE1/DDP cells transfected with Notch1 siRNA (images acquired at 100× magnification). Right panel: quantification of gap closure to calculate the healing

percentages (Mean ± SEM, *P<0.05, compared to siControl). C. Left panel: Transwell Boyden chamber assays to determine migratory and invasive potential of HNE1/DDP cells transfected with Notch1 siRNA (images acquired at 200× magnification). Right panel: Quantification of migrated and invaded cells. (Mean ± SEM, *P<0.05, compared to siControl).

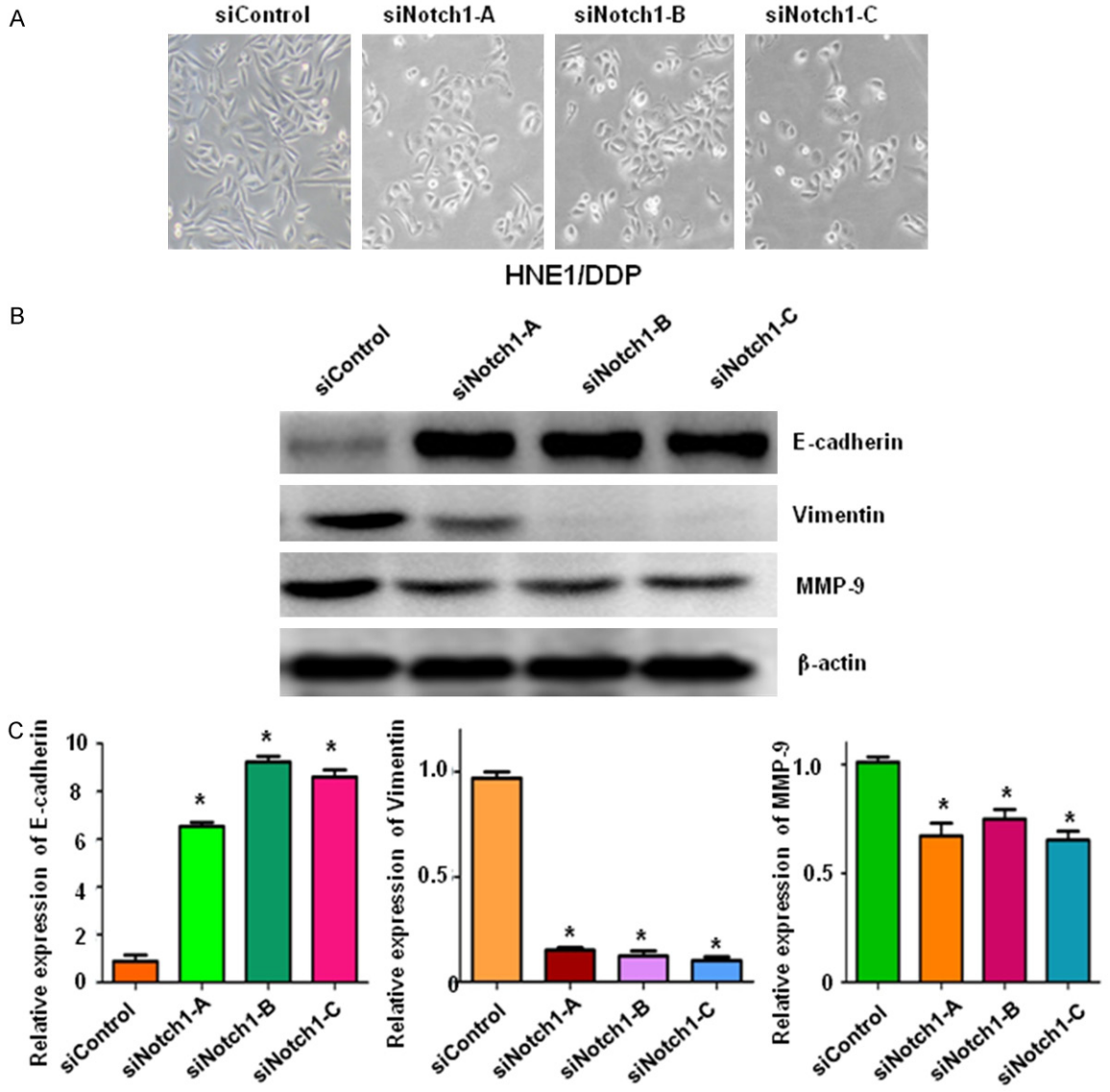

Figure 5. Knockdown of Notch1 reverses EMT in HNE1/DDP cells. A. Cell morphology of HNE1/DDP cells following Notch1 siRNA transfection (images acquired at 200× magnification). B. Western blot analysis demonstrates that transfection of Notch1 siRNA in HNE1 cells enhances E-cadherin protein abundance but reduces vimentin and MMP9 abundance. C. qRT-PCR analysis demonstrates that transfection of Notch1 siRNA in HNE1 cells up-regulates E-cadherin expression, whereas vimentin and MMP9 were down-regulated. mRNA was normalized to GAPDH (mean ± SEM, *P<0.05, compared to siControl).

HNE1/DDP cells. To further validate the role of miR-10b and Notch1 in EMT regulation, we depleted Notch1 in HNE1 cells transfected with miR-10b. We observed that depletion of Notch1 blocked the effect of ectopic miR-10b on EMT protein expression, migration and invasion (**Figure 6A-D**). Consistent with a role for the miR-10b/KLF4/Notch1 pathway in regulating EMT, ectopic expression of Notch1 rescued EMT, migration and invasion in HNE1/DDP cells treated with miR-10b inhibitors (**Figure 7A-D**). These findings reveal that Notch1 mediates miR-

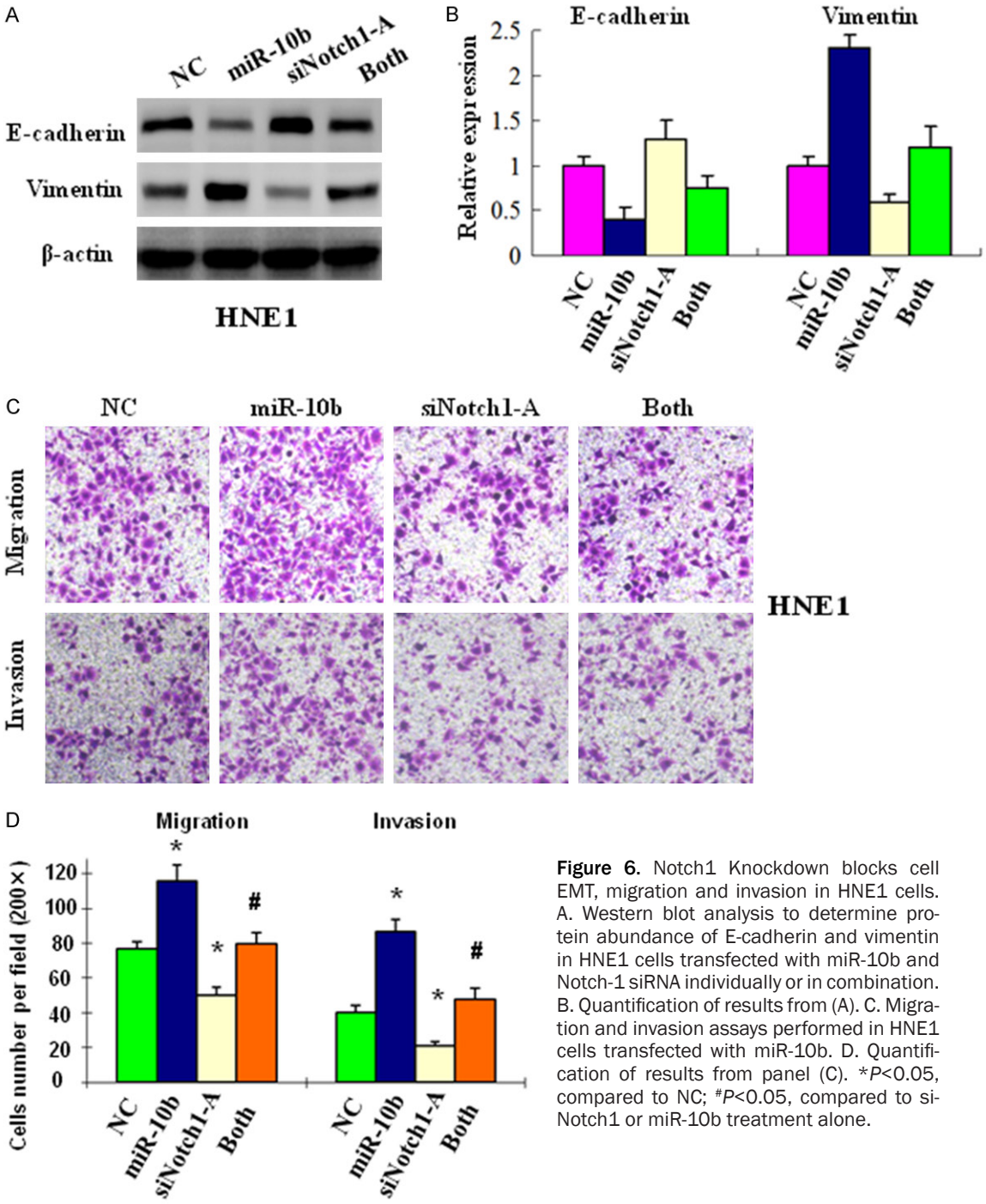

Figure 6. Notch1 Knockdown blocks cell EMT, migration and invasion in HNE1 cells. A. Western blot analysis to determine protein abundance of E-cadherin and vimentin in HNE1 cells transfected with miR-10b and Notch-1 siRNA individually or in combination. B. Quantification of results from (A). C. Migration and invasion assays performed in HNE1 cells transfected with miR-10b. D. Quantification of results from panel (C). **P*<0.05, compared to NC; #*P*<0.05, compared to si-Notch1 or miR-10b treatment alone.

10b regulation of EMT in HNE1 cells through targeting KLF4.

Discussion

Chemotherapy is an important therapeutic option for most cancer patients; however, the development of chemoresistance is a major limitation that leads to tumor recurrence and further progression [18]. Although the mechanisms responsible for chemoresistance have been investigated intensely over the past 50 years, the molecular mechanisms leading to drug resistance are complex and remain largely unknown [19]. Increasing evidence suggests a molecular and phenotypic association between chemoresistance and acquisition of an EMT phenotype by cancer cells. Previously, we dem-

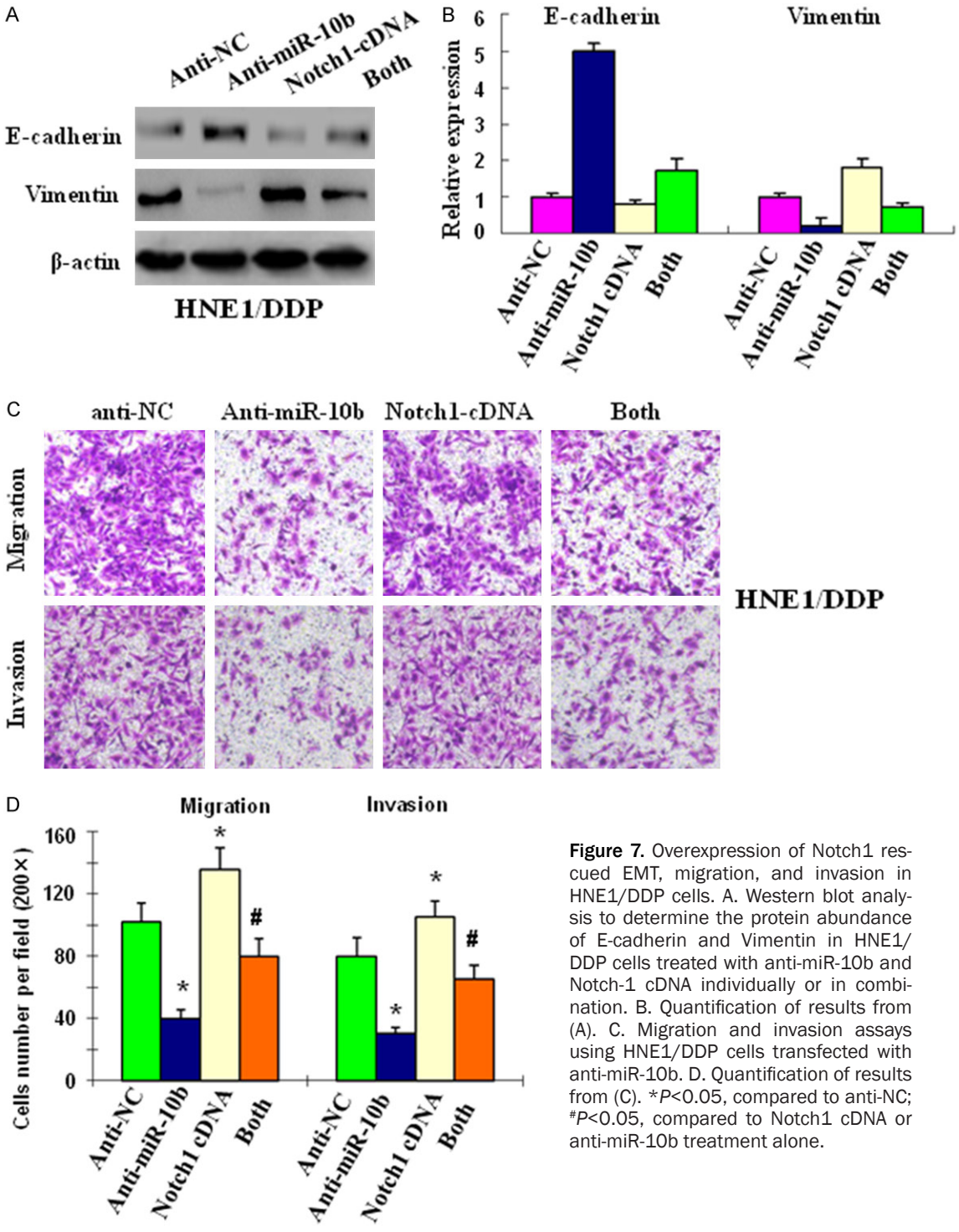

Figure 7. Overexpression of Notch1 rescued EMT, migration, and invasion in HNE1/DDP cells. A. Western blot analysis to determine the protein abundance of E-cadherin and Vimentin in HNE1/DDP cells treated with anti-miR-10b and Notch-1 cDNA individually or in combination. B. Quantification of results from (A). C. Migration and invasion assays using HNE1/DDP cells transfected with anti-miR-10b. D. Quantification of results from (C). **P*<0.05, compared to anti-NC; #*P*<0.05, compared to Notch1 cDNA or anti-miR-10b treatment alone.

onstrated that the development of resistance to cisplatin (DDP) in NPC cells is accompanied by inducible EMT-like changes and increased metastatic potential in *vitro* [20].

Recent evidence suggests that the expression of specific microRNAs (miRNAs) is altered in chemoresistant cells, leading to the dysregulation of expression of many oncogenes and tumor suppressor genes [21, 22]. The mechanisms by which miRNAs are dysregulated in cancer are complex and may involve genetic and epigenetic abnormalities as well as the altered activity of certain transcription factors

[23]. For example, miR-10b has been shown to play a critical role in tumorigenesis, where a TWIST/miR-10b/HOXD10/MMP14 signaling pathway is essential for glioma cell invasion [24]. Recently, it was reported that the stability and activity of the HIF1 protein is markedly increased in breast cancer cells in a CCN5/WISP2-deficient microenvironment. This ultimately leads to an increase in TWIST1 mediated miR-10b expression as well as the migration and invasion of these cells [25]. CCN5/WISP2-induced inhibition of miR-10b expression in breast cancer cells is mediated through the inhibition of the JNK-HIF1A-TWIST1 signaling pathway [26].

While it is becoming increasingly clear that miRNAs are key modulators of chemoresistance and EMT in many types of cancers [27], few reports have been published revealing their roles, or the role of miR-10b specifically, in cisplatin resistance. EMT is a key process driving cancer metastasis and the loss of E-cadherin and increase in vimentin expression are considered to be the most important molecular markers of EMT [28]. Recent studies have revealed that miRNAs act as crucial modulators of EMT through the regulation of E-cadherin and other molecules such as vimentin and ZEB. For example, miR-200a, miR-200b, and miR-200c (miR-200 family) were down-regulated in gemcitabine resistant pancreatic cancer cells, which acquire an EMT-like phenotype. Members of the miR-200 family have been shown to inhibit EMT by targeting ZEB1 and SIP1 [29, 30]. miR-205 was also reported to be down-regulated along with ZEB1 and ZEB2 during EMT in epithelial breast cancer cells [31]. Moreover, re-expression of miR-200b in EMT-type cells resulted in the reversal of the EMT phenotype through the induction of ZEB1, ZEB2, and Slug [32]. Our study has identified that miR-10b is up-regulated in HNE1/DDP cells, suggesting the possibility that miR-10b plays an important role in drug resistance. Our results further indicate that overexpression of miR-10b could promote invasion, migration, and the acquisition of EMT in HNE1 cells through decreased E-cadherin expression and increased vimentin and MMP9 expression. In contrast, inhibition of miR-10b reversed EMT in HNE1/DDP cells through increased E-cadherin expression and decreased vimentin and MMP9 expression. These findings demonstrated that miR-10b governs drug resistance partly through regulation of EMT.

Next, we explored the underlying mechanisms involved in the regulation of EMT by miR-10b. Bioinformatic prediction tools indicated that KLF4 is a putative target of miR-10b [33]. KLF4 is a transcription factor involved in cell cycle regulation, apoptosis, and differentiation [34]. Its expression increases in response to DNA damage, serum deprivation, and contact inhibition. Recently, miR-10b was shown to promote migration and invasion through regulation of KLF4 in human esophageal cancer cell lines [15]. KLF4 is a direct target of miR-10b that has been reported to suppress cancer cell migration and invasion [35]. Specifically, KLF4 has been shown to negatively regulate EMT in GI cancers. Down-regulation of KLF4 is required for EMT, cell migration, and for the induction of apoptosis [36]. Consistently, we also identified that miR-10b targeted KLF4 levels in human NPC cells. Together, these results indicate that miR-10b may regulate EMT by targeting KLF4 in human NPC cells.

Emerging evidence suggests that KLF4 inhibits the Notch signaling pathway [17, 37, 38]. In line with these reports, we found that Notch1 expression is higher in HNE1/DDP cells, which have low expression of KLF4. Previous reports showed that Notch1 expression is associated with an EMT phenotype in pancreatic cancer and other tumors [10, 39]. In addition, activation of Notch1 promotes the invasion and colony formation ability of gastric cancer [40]. Consistently, we observed that depletion of Notch1 inhibited cell migration and invasion and reversed EMT in HNE1/DDP cells. Altogether, miR-10b over-expression or inhibition controlled the levels of activated Notch1, regulated in part through miR-10b targeting KLF4. More importantly, depletion of Notch1 blocked EMT, migration and invasion in HNE1 cells transfected with miR-10b, whereas overexpression of Notch1 rescued EMT, migration and invasion in HNE1/DDP cells treated with anti-miR-10b. Our results suggest a critical role for Notch1 in miR-10b-mediated EMT in HNE1 cells.

In summary, we have demonstrated that miR-10b regulates EMT by modulating KLF4 and subsequent Notch1 expression, which ultimately affects the invasion and migration capabilities of NPC cells (**Figure 8**). Our study reveals a

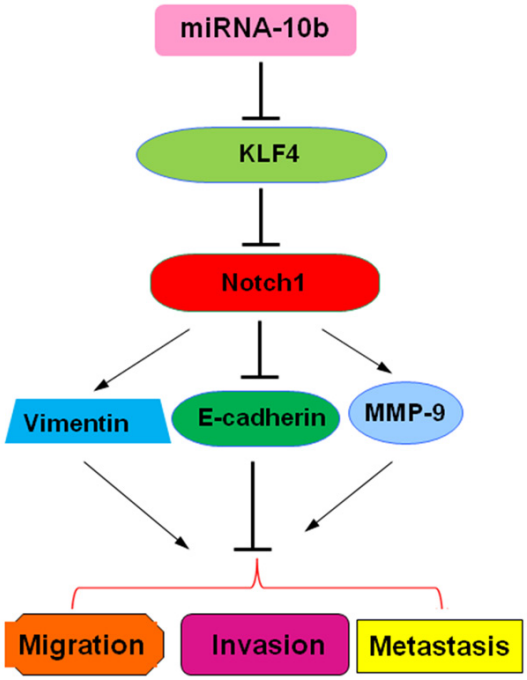

Figure 8. A schematic illustration of the signaling network showing how miR-10b promotes cell migration and invasion.

direct role and novel mechanism of miR-10b in reversing both the EMT phenotype and resistance to DDP. This information may be useful for developing a new therapy for treatment of NPC in the future. However, further study of the molecular mechanisms underlying metastasis of NPC, as well as identifying new therapeutic targets and preventing the recurrence of human nasopharyngeal carcinoma are the important goals for the future.

Acknowledgements

This work was supported by the National Natural Science Foundation of China (81372899, 81172087, and 81572936). This work was also supported by a project funded by the priority academic program development of Jiangsu higher education institutions.

Disclosure of conflict of interest

None.

Address correspondence to: Zhiwei Wang, Department of Pathology, Beth Israel Deaconess Medical Center, Harvard Medical School, Boston, MA 02215, USA. E-mail: zwang6@bidmc.harvard.edu; Chenchen Jiang, Priority Research Center for Cancer Research, University of Newcastle, Newcastle, NSW 2308, Australia. E-mail: chenchen_jiang@newcastle.edu.au; Hao Liu, Faculty of Pharmacy, Bengbu Medical College, Anhui Engineering Technology Research Center of Biochemical Pharmaceuticals, Bengbu 233030, Anhui, P. R. China. E-mail: liuhao6886@foxmail.com

References

[1] Jemal A, Bray F, Center MM, Ferlay J, Ward E and Forman D. Global cancer statistics. CA Cancer J Clin 2011; 61: 69-90.

[2] Chen QY, Wen YF, Guo L, Liu H, Huang PY, Mo HY, Li NW, Xiang YQ, Luo DH, Qiu F, Sun R, Deng MQ, Chen MY, Hua YJ, Guo X, Cao KJ, Hong MH, Qian CN and Mai HQ. Concurrent chemoradiotherapy vs radiotherapy alone in stage II nasopharyngeal carcinoma: phase III randomized trial. J Natl Cancer Inst 2011; 103: 1761-1770.

[3] Bartel DP. MicroRNAs: target recognition and regulatory functions. Cell 2009; 136: 215-233.

[4] Ambros V. MicroRNA pathways in flies and worms: growth, death, fat, stress, and timing. Cell 2003; 113: 673-676.

[5] Wang Z, Li Y, Ahmad A, Azmi AS, Kong D, Banerjee S and Sarkar FH. Targeting miRNAs involved in cancer stem cell and EMT regulation: An emerging concept in overcoming drug resistance. Drug Resist Updat 2010; 13: 109-118.

[6] Iorio MV and Croce CM. Causes and consequences of microRNA dysregulation. Cancer J 2012; 18: 215-222.

[7] Bracken CP, Gregory PA, Khew-Goodall Y and Goodall GJ. The role of microRNAs in metastasis and epithelial-mesenchymal transition. Cell Mol Life Sci 2009; 66: 1682-1699.

[8] Colas E, Pedrola N, Devis L, Ertekin T, Campoy I, Martinez E, Llaurado M, Rigau M, Olivan M, Garcia M, Cabrera S, Gil-Moreno A, Xercavins J, Castellvi J, Garcia A, Ramon y Cajal S, Moreno-Bueno G, Dolcet X, Alameda F, Palacios J, Prat J, Doll A, Matias-Guiu X, Abal M and Reventos J. The EMT signaling pathways in endometrial carcinoma. Clin Transl Oncol 2012; 14: 715-720.

[9] Li Y, Ma J, Qian X, Wu Q, Xia J, Miele L, Sarkar FH and Wang Z. Regulation of EMT by Notch signaling pathway in tumor progression. Curr Cancer Drug Targets 2013; 13: 957-962.

[10] Bao B, Wang Z, Ali S, Kong D, Li Y, Ahmad A, Banerjee S, Azmi AS, Miele L and Sarkar FH. Notch-1 induces epithelial-mesenchymal transition consistent with cancer stem cell phenotype in pancreatic cancer cells. Cancer Lett 2011; 307: 26-36.

[11] Wang Z, Azmi AS, Ahmad A, Banerjee S, Wang S, Sarkar FH and Mohammad RM. TW-37, a small-molecule inhibitor of Bcl-2, inhibits cell growth and induces apoptosis in pancreatic cancer: involvement of Notch-1 signaling pathway. Cancer Res 2009; 69: 2757-2765.
[12] Zhang G, Zhu H, Wang Y, Yang S, Liu M, Zhang W, Quan L, Bai J, Liu Z and Xu N. Kruppel-like factor 4 represses transcription of the survivin gene in esophageal cancer cell lines. Biol Chem 2009; 390: 463-469.
[13] Luo A, Kong J, Hu G, Liew CC, Xiong M, Wang X, Ji J, Wang T, Zhi H, Wu M and Liu Z. Discovery of Ca2+-relevant and differentiation-associated genes downregulated in esophageal squamous cell carcinoma using cDNA microarray. Oncogene 2004; 23: 1291-1299.
[14] Yang Y, Goldstein BG, Chao HH and Katz JP. KLF4 and KLF5 regulate proliferation, apoptosis and invasion in esophageal cancer cells. Cancer Biol Ther 2005; 4: 1216-1221.
[15] Tian Y, Luo A, Cai Y, Su Q, Ding F, Chen H and Liu Z. MicroRNA-10b promotes migration and invasion through KLF4 in human esophageal cancer cell lines. J Biol Chem 2010; 285: 7986-7994.
[16] Cui J, Shi M, Quan M and Xie K. Regulation of EMT by KLF4 in gastrointestinal cancer. Curr Cancer Drug Targets 2013; 13: 986-995.
[17] Hale AT, Tian H, Anih E, Recio FO 3rd, Shatat MA, Johnson T, Liao X, Ramirez-Bergeron DL, Proweller A, Ishikawa M and Hamik A. Endothelial Kruppel-like factor 4 regulates angiogenesis and the Notch signaling pathway. J Biol Chem 2014; 289: 12016-12028.
[18] Latifi A, Luwor RB, Bilandzic M, Nazaretian S, Stenvers K, Pyman J, Zhu H, Thompson EW, Quinn MA, Findlay JK and Ahmed N. Isolation and characterization of tumor cells from the ascites of ovarian cancer patients: molecular phenotype of chemoresistant ovarian tumors. PLoS One 2012; 7: e46858.
[19] Broxterman HJ, Gotink KJ and Verheul HM. Understanding the causes of multidrug resistance in cancer: a comparison of doxorubicin and sunitinib. Drug Resist Updat 2009; 12: 114-126.
[20] Zhang P, Liu H, Xia F, Zhang QW, Zhang YY, Zhao Q, Chao ZH, Jiang ZW and Jiang CC. Epithelial-mesenchymal transition is necessary for acquired resistance to cisplatin and increases the metastatic potential of nasopharyngeal carcinoma cells. Int J Mol Med 2014; 33: 151-159.
[21] Galluzzi L, Morselli E, Vitale I, Kepp O, Senovilla L, Criollo A, Servant N, Paccard C, Hupe P, Robert T, Ripoche H, Lazar V, Harel-Bellan A, Dessen P, Barillot E and Kroemer G. miR-181a and miR-630 regulate cisplatin-induced cancer cell death. Cancer Res 2010; 70: 1793-1803.
[22] Rui W, Bing F, Hai-Zhu S, Wei D and Long-Bang C. Identification of microRNA profiles in docetaxel-resistant human non-small cell lung carcinoma cells (SPC-A1). J Cell Mol Med 2010; 14: 206-214.
[23] Dong CG, Wu WK, Feng SY, Wang XJ, Shao JF and Qiao J. Co-inhibition of microRNA-10b and microRNA-21 exerts synergistic inhibition on the proliferation and invasion of human glioma cells. Int J Oncol 2012; 41: 1005-1012.
[24] Sun L, Yan W, Wang Y, Sun G, Luo H, Zhang J, Wang X, You Y, Yang Z and Liu N. MicroRNA-10b induces glioma cell invasion by modulating MMP-14 and uPAR expression via HOXD10. Brain Res 2011; 1389: 9-18.
[25] Banerjee SK and Banerjee S. CCN5/WISP-2: A micromanager of breast cancer progression. J Cell Commun Signal 2012; 6: 63-71.
[26] Haque I, Banerjee S, Mehta S, De A, Majumder M, Mayo MS, Kambhampati S, Campbell DR and Banerjee SK. Cysteine-rich 61-connective tissue growth factor-nephroblastoma-overexpressed 5 (CCN5)/Wnt-1-induced signaling protein-2 (WISP-2) regulates microRNA-10b via hypoxia-inducible factor-1alpha-TWIST signaling networks in human breast cancer cells. J Biol Chem 2011; 286: 43475-43485.
[27] Schoof CR, Botelho EL, Izzotti A and Vasques Ldos R. MicroRNAs in cancer treatment and prognosis. Am J Cancer Res 2012; 2: 414-433.
[28] Sun Y, Shen S, Liu X, Tang H, Wang Z, Yu Z, Li X and Wu M. miR-429 inhibits cells growth and invasion and regulates EMT-related marker genes by targeting Onecut2 in colorectal carcinoma. Mol Cell Biochem 2014; 390: 19-30.
[29] Paterson EL, Kazenwadel J, Bert AG, Khew-Goodall Y, Ruszkiewicz A and Goodall GJ. Down-regulation of the miRNA-200 family at the invasive front of colorectal cancers with degraded basement membrane indicates EMT is involved in cancer progression. Neoplasia 2013; 15: 180-191.
[30] Gregory PA, Bert AG, Paterson EL, Barry SC, Tsykin A, Farshid G, Vadas MA, Khew-Goodall Y and Goodall GJ. The miR-200 family and miR-205 regulate epithelial to mesenchymal transition by targeting ZEB1 and SIP1. Nat Cell Biol 2008; 10: 593-601.
[31] Lee JY, Park MK, Park JH, Lee HJ, Shin DH, Kang Y, Lee CH and Kong G. Loss of the polycomb protein Mel-18 enhances the epithelial-mesenchymal transition by ZEB1 and ZEB2 expression through the downregulation of miR-205 in breast cancer. Oncogene 2014; 33: 1325-35.
[32] Kong D, Li Y, Wang Z, Banerjee S, Ahmad A, Kim HR and Sarkar FH. miR-200 regulates

PDGF-D-mediated epithelial-mesenchymal transition, adhesion, and invasion of prostate cancer cells. Stem Cells 2009; 27: 1712-1721.

[33] Lin J, Teo S, Lam DH, Jeyaseelan K and Wang S. MicroRNA-10b pleiotropically regulates invasion, angiogenicity and apoptosis of tumor cells resembling mesenchymal subtype of glioblastoma multiforme. Cell Death Dis 2012; 3: e398.

[34] Mao L, Zhang Y, Deng X, Mo W, Yu Y and Lu H. Transcription factor KLF4 regulates microRNA-544 that targets YWHAZ in cervical cancer. Am J Cancer Res 2015; 5: 1939-1953.

[35] Xiao H, Li H, Yu G, Xiao W, Hu J, Tang K, Zeng J, He W, Zeng G, Ye Z and Xu H. MicroRNA-10b promotes migration and invasion through KLF4 and HOXD10 in human bladder cancer. Oncol Rep 2014; 31: 1832-1838.

[36] Tiwari N, Meyer-Schaller N, Arnold P, Antoniadis H, Pachkov M, van Nimwegen E and Christofori G. Klf4 is a transcriptional regulator of genes critical for EMT, including Jnk1 (Mapk8). PLoS One 2013; 8: e57329.

[37] Lambertini C, Pantano S and Dotto GP. Differential control of Notch1 gene transcription by Klf4 and Sp3 transcription factors in normal versus cancer-derived keratinocytes. PLoS One 2010; 5: e10369.

[38] Liu Z, Teng L, Bailey SK, Frost AR, Bland KI, LoBuglio AF, Ruppert JM and Lobo-Ruppert SM. Epithelial transformation by KLF4 requires Notch1 but not canonical Notch1 signaling. Cancer Biol Ther 2009; 8: 1840-1851.

[39] Xie M, Zhang L, He CS, Xu F, Liu JL, Hu ZH, Zhao LP and Tian Y. Activation of Notch-1 enhances epithelial-mesenchymal transition in gefitinib-acquired resistant lung cancer cells. J Cell Biochem 2012; 113: 1501-1513.

[40] Yeh TS, Wu CW, Hsu KW, Liao WJ, Yang MC, Li AF, Wang AM, Kuo ML and Chi CW. The activated Notch1 signal pathway is associated with gastric cancer progression through cyclooxygenase-2. Cancer Res 2009; 69: 5039-5048.